Article

Not peer-reviewed version

Experimental Early Stimulation of Bone Tissue Neo-Formation for Critical Size Elimination Defects in the Maxillofacial Region

Nadezhda N. Patlataya , Igor Nikolaevich Bolshakov * , Anatoli A. Levenets , Nadezhda N. Medvedeva , Mariya A. Cherkashina

Posted Date: 14 August 2023

doi: 10.20944/preprints202308.1032.v1

Keywords: experimental critical size bone defect; maxillofacial area; modified chitosan; early bone formation; morphometry; rats

Article

Experimental Early Stimulation of Bone Tissue Neo-Formation for Critical Size Elimination Defects in the Maxillofacial Region

N.N. Patlataya [1], I.N. Bolshakov [2,*], A.A. Levenets [2], N.N. Medvedeva [3] and M.A. Cherkashina [3]

[1] Institute of Medicine and Biology
[2] Voino-Yasenetsky Krasnoyarsk State Medical University
[3] Профессор Красноярский государственный медицинский университет имени В. Ф. Войно-Ясенецкого
* Correspondence: bol.bol@mail.ru

Abstract: A biomaterial is proposed for closing extensive bone defects in the maxillofacial region. The composition of the biomaterial includes high molecular weight chitosan, chondroitin sulfate, hyaluronate, heparin, alginate and inorganic nanostructured hydroxyapatite. The purpose of the study is to demonstrate morphological and histological early signs of reconstruction of a bone cavity of a critical size. The studies were carried out on 84 white female rats weighing 200 g. The control group of animals consisted of 44 individuals, the study group - 40. In all animals, three-walled bone defects 0.5 cm in size were applied subperiosteally in the region of the angle of the lower jaw and filled in the experimental group with a gel mass of chitosan -alginate-hydroxyapatite (CH-SA-HA). In control animals, the bone cavities were filled with an auto-blood clot. The follow-up periods were 3.5.7 days, 2.3.4.6.8 and 10 weeks. The chitosan construct after implantation actively replaced defects early with the formation of a full-fledged new bone tissue compared to control animals. Morphological analysis of the walls of the bone defect on the 7th day showed signs of the formation of spongy bone tissue, after two weeks - a pronounced increase in bone volume ($P<0.01$), after 6 weeks after surgery, the closure of the defect was 70-80%, after 8 weeks - 100% without disturbing bone morphology with a high degree of mineralization. The use of modified chitosan after filling eliminates bone defects of critical size in the maxillofacial region, reveals early signs of bone neoformation, and serves as a promising material in reconstructive dentistry.

Keywords: experimental critical size bone defect; *maxillofacial area;* modified chitosan; early bone formation; morphometry; rats

1. Introduction

Restoration of bone defects in the maxillofacial region after surgical interventions is a well-known topical problem. The successive stages of bone regeneration: inflammation, formation of a soft callus, and later hard tissue, and finally remodeling of the newly formed bone often constitute a long-term chronic process. In the field of applied dentistry, researchers offer a variety of plastic materials that can cause an osteogenesis reaction upon contact with a bone, replacing bone tissue defects. The inclusion of low molecular weight bioregulatory peptides in the composition of chitosan structures stimulates the early appearance of signs of reparative osteogenesis, which indicates a rather high osteoaffinity of the compositions with the formation of a dense fragment of bone and bone marrow, as well as osteons, starting from the 30th day, by more than 40% [1]. However, it is known that in a large area of bone damage, the actual physiological repair is not able to eliminate the defect on its own, and the use of many polymer structures does not have the expected effect of regeneration [2–4]. In the absence of automaterial, the creation of functional bone using highly biocompatible substrates capable of self-organization of molecular architecture with high biocompatibility and the presence of exogenous growth factors can close a large bone defect [5,6]. From this point of view, the same chitosan construct with a high degree of purification and deacetylation with a glomerular

 doi:10.20944/preprints202308.1032.v1

conformation of the molecule up to nanosizes in reaction with chondroitin sulfate, hyaluronate, heparin, and alginate can be a promising starting material [7]. The concept of using the proposed polysaccharide construct is to significantly increase its functionality, on the one hand, as a system for transferring target ingredients through the compartment in the osteogenic process, and on the other hand, in the implantation of a building material during the formation of a newly formed bone and obtaining signs of early bone formation [8]. Histological and immunohistochemical studies demonstrate that chitosan matrices create neovascularization conditions in vivo at the early stages of implantation and are suitable for tissue engineering [9]. In cases of early regeneration of bone tissue in the elimination of defects of a critical size, the management of angiogenesis is a mandatory process and is accompanied by the binding and release of angiogenic growth factors [10,11], early formation of a highly vascularized periodontium proper [12]. This indicates the conjugation of the processes of osteogenesis and angiogenesis [13]. Additional protonation of the NH2 group in the chitosan molecule, for example, with the help of weak ascorbic acid, makes it possible to increase the efficiency of controlling angiogenic reactions in the periodontium [14]. Physical cross-linking of biopolymers to obtain soft three-dimensionally structured hydrogels makes it possible to use them for tissue engineering [15] as systems for delivering hyaluronic acid and chondroitin sulfate, starch and cellulose, or their chemical derivatives to the area of damaged maternal bone tissue [16, 17]. With long-term bone regeneration in the maxillofacial region, it is important to control the preservation of the structural integrity and function of the hydrogel matrix until the formation of new bone tissue with the transfer of the entire matrix to the area of the bone defect. It is very important that early active osteogenesis proceeds under conditions of an anti-inflammatory reaction, since the chitosan structure forms electrostatic and concentration gradients for cells, metabolites and water and leads to their movement towards the polymer, which reduces the degree of inflammation both at the site of the polymer dislocation and outside [18].

2. Materials and Methods

The work was performed following ethical principles established by the European Convention for the Protection of Vertebrate Animals used for Experimental and Other Scientific Purposes (Strasbourg, 18 March 1986, adopted on 15 June 2006). All manipulations with the animals were performed following the regulations specified in the Guide for the Care and Use of Laboratory Animals (National Research Council, 2011). The work was approved: complex scientific theme No. 01201362513 (2013/01/01 – 2021/01/01) "Fundamental and applied scientific and technical developments of nano-level biopolymer structures and technologies for their production for use in cell and tissue engineering in socially significant human diseases"; Section "Dentistry": Obtaining, testing and introduction into clinical practice of cell substrates for direct implantation into hard and soft tissues of the periodontium in order to reconstruct the tissues of the maxillofacial region, eliminate the causes of the formation of degeneration zones and the formation of periodontolysis zones; Research topic: "Restoration of the structure of the bone tissue of the maxillofacial region using polysaccharide polymers with extensive traumatic defects in conditions of subcompensated diabetes mellitus." Bioethical Commission for Working with Animals by the Ethics Committee of the Voino-Yasenetsky Krasnoyarsk State Medical University of the Ministry of Health Russian Federation (Protocol No2 of 10/28/2019).

2.1. Composition of CH-SA-HA Construction

The Developer is SBEU HPT Krasnoyarsk State Medical University, Russia. Gel mass chitosan-alginate-hydroxyapatite (CH-SA-HA) containing a 2% solution of chitosan ascorbate (CH) (dissolution of the polymer in ascorbic solution acid in a ratio of 1: 1.5) with a molecular weight of 695 kDa and a degree of deacetylation of 95% (a triply purified chitosan obtained in Vostok-Bor-1, Dal'negorsk, Russia; Specifications (No 9289-067-004721224-97), including, per 1 g of dry chitosan ascorbate, 5-100 mg of sodium chondroitin sulfate (Sigma), 10-100 mg of sodium hyaluronate (Sigma), 2,5-5 mg of heparin sulfate (Russia, Pharm.Art. (No 42-1327-99), 110 mcg/d serum growth factors in cattle "adgelon" (SLL "Endo-Pharm-A", Moscow region, Schcholkovo, Russia, Specifications (No 113910- 001-01897475-97), 4% sodium alginate (Pharm.Art. No 42-3383-97 or Specifications (No 15-544-83; Arkhangelsk algal plant. Co), including 50 wt% amorphous hydroxyapatite (5-20 nm, Russia, Pharm.Art. No 42-3790- 99 or GOST 12.1.007-76)(SA-HA), in the ratio of chitosan ascorbate and

sodium alginate 1:1(CH-SA-HA)[19]. The gel mass was placed into vials in a volume of 2 ml, lyophilized and sterilized electronically.

7.2 grams of chitosan are added to the prepared solution of ascorbic acid (Pharm.Art. No 42-2668-95) with stirring at a temperature of + 20-25 ° C, the mass is stirred for 4-5 hours until the chitosan is completely dissolved. Aqueous solutions of sodium salts of chondroitin sulfuric acid, hyaluronic acid, and heparin are successively added to the resulting 4% chitosan solution with constant slow stirring using a magnetic stirrer in a total volume equal to the volume of chitosan ascorbate. The introduction of each subsequent ingredient is carried out after the homogeneous mixing of the previous one with the chitosan gel. As a result, a 2% chitosan polyionic complex is obtained. Next, a 4% aqueous solution (gel) of sodium alginate is prepared, 50% (by dry weight) of hydroxyapatite is added. The finished chitosan solution is thoroughly mixed with the sodium alginate solution using a high-speed mixer.

2.2. Experimental Animals

The conditions of biological test systems in the CDI CI correspond to Guide for the Care and Use of Laboratory Animals, 8th edition, 2011, NRC, USA (Manual on the content and use of laboratory animals, 8th edition, 2011, national research Committee, USA). The maintenance of animals in individually ventilated cells from polysulfone Sealsafe, 461×274×228 mm (production TECHNIPLAST.P. A.). The rooms, which contain biological test systems, controlled temperature (18-24 C), humidity (30-70%), illumination (12/12 h), the multiplicity of air (XII without recirculation). Control of climatic parameters is carried out in accordance with the SOP "control of climatic parameters in the premises of the vivarium." The distribution of feed and water is carried out at a fixed time, the change of litter is made once a week in accordance with the SOP "preparation of cells for biological test systems. Marking. Change of bedding, feed, water".

2.3. Modeling Defects of the Critical Size of the Mandibular Angle in Rats

The study was conducted on 84 female Wistar rats weighing 200 g. Laboratory animals were divided into 1 control and 1 study group. Each group was subjected to a morphometric study at 3.5 days, 1,2,3,4,6,8 and 10 weeks. The study group included 40 animals, in which an extensive defect in the lower jaw was modeled, followed by the filling of the bone cavity with a polymeric construct: chitosan ascorbate-sodium alginate-hydroxyapatite ("CH-SA-HA"). The control group included 44 animals with an identical bone cavity filled with a natural intraoperative blood clot at the same time of observation. Anesthesia was performed using a mixture of tiletamine/zolazepam at a dose of 2 mg/rat (Zoletil 100, Vibrac, France) and xylazil (Rometar, Bioveta, Czech Republic) at a dose of 0.02 ml/rat in a ratio of 1:1. The mixture was injected in a volume of 0.5 ml intramuscularly, then the skin in the lower jaw area was treated using an aqueous solution of chlorhexidine, an incision was made on the lower jaw in the area of the masticatory ridge 1.5-2 cm long. masseter and periosteum, a rounded three-wall defect 5 mm in size was applied on the masticatory ridge with a dental spherical burr. While burring, the bone was cooled with an aqueous 0.2% chlorhexidine solution (series CHG-013/17 J. Amphrey Laboratories, India). The cavity of the bone defect was dried with tampons and filled with CH-SA-HA lyophilic mass or auto-blood clot), the defect was closed with periosteum, and the skin was sutured with separate 5.0 monofilament sutures. The wound was treated with 1% aqueous solution of chlorhexidine. In order to prevent the development of the inflammatory process, all animals were injected intramuscularly with the antibacterial drug Ceftriaxone at a dose of 8 mg/rat, the antihistamine drug Suprastin at a dose of 0.1 mg/rat. Within three days after surgery, the animals received Tramadol 2.5 mg 2 times a day. During the first day, access to water was provided. Feeding was carried out 24 hours after the operation with an exclusively liquid mixture "Polyproten-Nefro" using soy protein Supra 760 (USA) (LLC "Protenfarma", Russia) for 3 days. Medical support was provided by a broad-spectrum antibiotic (ceftriaxone at a dose of 8 mg/rat), antispasmodics, and vasodilators. The sutures were removed on the 7th day after surgery.

2.4. Morphological Analysis of Bone Tissue

The mandibles of the animals were placed in a 10% solution of buffered formalin, then fragments of the bodies of the mandibles were separated in the area of the postoperative defect with the capture of unchanged bone along the perimeter for 5 mm and placed in the decalcifying solution "Trilon B"

for a period of 24-48 hours. The decalcified fragments were dehydrated in increasing concentrations of isopropyl alcohol and embedded in paraffin wax. On a MicroTec CUT4050 microtome, serial sections (20-25 sections) of 4-5 μm in thickness were made in the transverse plane (relative to the animal's body) through the entire area of the bone defect in the area of its outer and inner walls. Sections were stained with hematoxylin-eosin and picrofuchsin according to van Gieson. The morphological study was carried out on an Olympus BX45 microscope with an Olympus DP 25 attachment for photo-video documentation and the Cell^D software package, as well as with scanning histological preparations in a FLASH 250 3D HISTECH histoscanner (Hungary) at a magnification of x100, x200, x400. Histo-morphometric evaluation was performed on digital micrographs, which were obtained using the software "Cell^D" and "NIS-Elements Document", while morphometric measurements were performed in the program "JMicroVision 1.2.7". Digital histological sections obtained as a result of scanning microprep-arations in a histoscanner were evaluated using the CaseViewer Ver.2.3 Build 2.3.9.99276 3D HISTECH software (Hungary).

Bone tissue recovery was assessed according to the following histomorphometric criteria: volumetric density of bone and connective tissue (BV (%), the percentage ratio of the volume occupied by bone structures to the total volume of the histological section); thickness of bone trabeculae (BTT (mm), the criterion stipulates that the bone trabecula is a thin plate, measurements were taken between the edges of the bone trabecula (5-8 measurements in relation to each trabecula with the calculation of the median); intertrabecular spaces (ITS (mm), the distance between the edges of the cancellous bone trabeculae, the calculation is made in accordance with the so-called parallel plate model: BV minus BTT (mm); volumetric density of osteoid and vessels (OS (%), the percentage ratio of the surface of bone trabeculae occupied by osteoid to the total bone surface); numerical density of inflammatory cell infiltrate (%) (fibroblasts, segmented leukocytes, histiocytes, giant multinucleated cells); bulk density of the implant (%); free bone surface area (FS (%), the percentage of the non-eroded surface of bone trabeculae and the surface not occupied by osteoblasts, osteoclasts to the total bone surface); area filled with osteoblastic cells of bone trabeculae (OBS, the percentage ratio of the surface of bone trabeculae occupied by osteoblasts to the total bone surface); eroded (osteoclastic) surface of bone trabeculae area (ES (%), the percentage ratio of the surface of bone trabeculae with the formation of gaps to the total bone surface, includes the surface occupied by osteoclasts. The numerical density of cell structures was measured as the number of cells in relation to the area of the field of view. The relative density of the measured structures was determined by the formula: RDS (%) = (Sa/St)*100, where Sa is the total area of all selected areas, St is the area of the digital image.

2.5. Statistical Analysis

Statistical analysis of data and the creation of graphic illustrations were carried out using the free software computing environment "R, version 4.2.1" and the programming language "R". The assessment of the obtained variables in relation to compliance with the normal (Gaussian) distribution was carried out on the basis of the Shapiro-Wilk test, as well as on the basis of the graphical method (Quantile-Quantile plot). Most of the variables obtained obeyed the normal distribution law, and the cases of deviation of the variables from the normal distribution were not pronounced. For variables deviating from the normal distribution, the following methods of data transformation were used to achieve compliance with the normal distribution: with right-sided (positive) skewness, square roots were taken from the obtained values, and in the case of left-sided (negative) skewness, the formula was used - $\sqrt{\max(x+1)-x}$, where "X" is the value obtained. Descriptive statistics of the obtained data were presented as median, 25% and 75% quartiles (Me[Q1;Q3]). During the choosing statistical tests for assessing the type I error (α) and the sensitivity of the criterion (1-β), parametric methods of statistical analysis were used: one-way analysis of variance (ANOVA), for paired comparisons of independent variables, Welch's t-test was used, for multiple comparisons, we used Bonferroni amendment. The presented variants of assessments were carried out taking into account the equality of variances, the variables under study, as well as taking into account the level of sensitivity of the criteria not lower than p=0.75. To assess the error of the first kind, taking into account the small volume of the studied samples, the threshold value p=0.01 was used.

Preprints (www.preprints.org) | NOT PEER-REVIEWED | Posted: 14 August 2023 doi:10.20944/preprints202308.1032.v1

3. Results

Morphological Analysis of Bone Tissue Restoration in the Defect Zone

Plain microscopy of histological preparations in the area of the postoperative defect of the lower jaws of healthy rats removed after 3 days of the experiment revealed extensive foci of hemorrhagic impregnation (Figure A.1) in combination with severe inflammatory infiltration and a clear predominance of segmented leukocytes. Among other cells of the inflammatory infiltrate, the presence of lymphocytes, histiocytes, fibroblasts and plasma cells was noted. There were also visualized signs of the formation of granulation tissue with a pronounced edematous extracellular matrix and numerous thin-walled capillaries. In histological preparations from the group with implanted "CH-SA-HA" biopolymer, along with the changes described above, abundant, diffusely distributed amphophilic granules of a foreign substance were determined. In histological preparations on the 5th and 7th days of the experiment, a similar microscopic picture was noted with an important feature, which was characterized by the appearance of eosinophilic "islands" of bone tissue formation with the presence of cubic and polygonal cells on the surfaces of cells with weakly basophilic cytoplasm and spherical nuclei - osteoblasts (Figure B.1). Single large cells with multiple spherical nuclei and homogeneous "foamy" cytoplasm - osteoclasts - were also detected. In some preparations, these cells were absent. In separate preparations on the 7th day of the experiment of both study groups, along with bone tissue, the formation of small areas of cartilage tissue was noted. In the walls of the bone defect, the migration of mesenchymal stromal cells towards the blood clot is typical in the earliest stages (Figure C.1). For the control group, after 1 week, only the filling of the bone cavity with immature connective tissue is typical (Figure D.1).

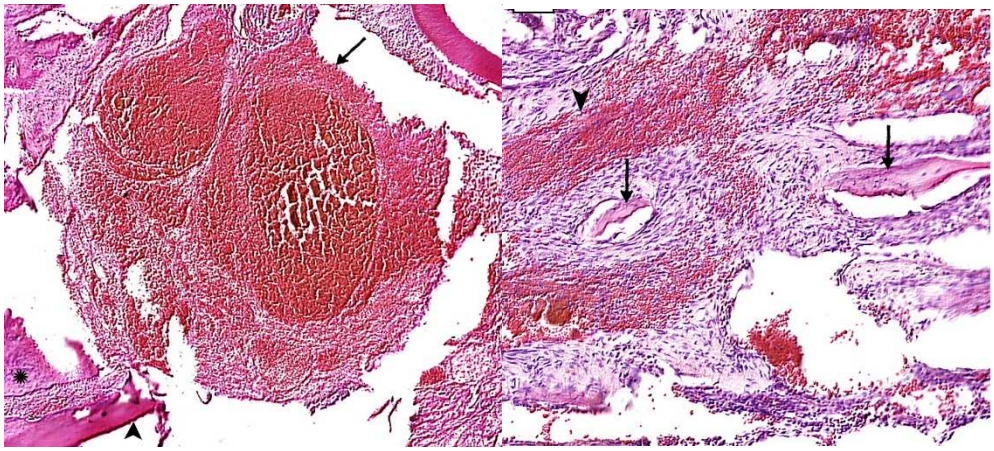

A.1 B.1

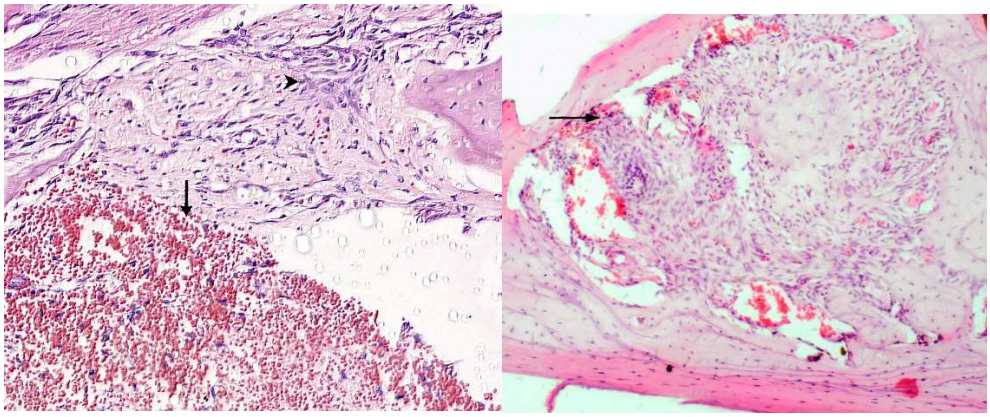

C.1 D.1

Figure 1. Regeneration of a bone defect in the lower jaw of healthy rats at the early stages of the experiment. A.1 - control group, day 3 of the experiment, a formed defect with a blood clot (↑), a periodontal ligament (*) and a cortical plate of the lower jaw (^) are visible, magnification x30; B.1 - CH-SA-HA group, day 7 of the experiment, islands of regenerating bone tissue (↑) in the area of hemorrhagic impregnation (^), x80

Preprints (www.preprints.org) | NOT PEER-REVIEWED | Posted: 14 August 2023 doi:10.20944/preprints202308.1032.v1

magnification; C.1 - CH-SA-HA group, day 3 of the experiment, there is no bone tissue at the site of the defect, mesenchymal stromal cells (^) migrate to the area of the blood clot (↑), with further differentiation into osteoblasts, x170 magnification; D.1 - control group, 7th day of the experiment, the bone defect is filled with immature connective tissue (↑), magnification x40. Hematoxylin-eosin staining.

The assessment of the numerical density of the inflammatory infiltrate was made per unit area - 0.043 mm2, which corresponded to the area of the field of view displayed on the monitor screen at x400 magnification. The presented histomorphometric criterion was not studied after the experiment period of 3 weeks due to the complete elimination of pathomorphological signs of inflammation. As shown in Table 1, in multiple comparisons using one-way analysis of variance, there was a significant influence of factors such as the timing of the experiment and group affiliation at each time interval of the experiment. Indicators of the numerical density of the inflammatory infiltrate in the early stages after surgery significantly increased daily in both studied groups ($p<0.01$), while in the group of animals with implanted biopolymer "CH-SA-HA" the objective indicator of cell infiltration from the 3rd to the 7th day of the experiment increased by 57% ($p<0.01$), while in the control group the same range of changes was only 36% ($p<0.01$). After 2 weeks of observation in both study groups, there was a more than twofold decrease in the volume of the numerical density of the inflammatory infiltrate ($p<0.01$). In pairwise comparisons, the numerical density of the inflammatory infiltrate in the experimental group was significantly lower ($P<0.01$) at all estimated time intervals of the experiment, except for the period of 3 weeks (Table 1). In pairwise comparisons, the digital values of the numerical density of the inflammatory infiltrate in the peripheral zone of the bone defect (experiment) were significantly lower by more than 2 times ($p<0.01$) compared with the values in the zone of the bone defect proper.

Table 1. Histomorphometric criteria for the repair of a bone defect in the lower jaw of rats (Me[25;75]).

Early dates

Experiment period	Area of mandibular defect		Defect periphery[1] Control + experience
	Experience CH-SA-HA[1]	Control Healing under a blood clot[1]	
Numerical density of inflammatory infiltrate (unit/0.043 mm²)			
3 day[1]	56,1[46,4;67,6]	67,4[57,6;72,1]**	9,3[7,9;9,7]**
5 day[1]	85,7[72,1;90,7]	93,7[86,1;99,4]**	14,6[13,4;15,7]**
7 day[1]	88,1[74,6;91,9]	91,4[81,5;99,4]**	11,3[10,1;12,3]**
Volumetric density of bone tissue (BV (%)			
5 day[1]	1,1[0,9;1,3]	1,1[0,8;1,5]	65,3[64,2;66,4]**
7 day[1]	15,1[13,0;16,7]	16,2[14,9;17,9]	66,5[65,6;68,8]**
Trabeculae thickness (mm)			
5 day[1]	0,04[0,03;0,05]	0,04[0,04;0,05]	0,15[0,15;0,16]**
7 day[1]	0,06[0,05;0,07]	0,06[0,05;0,06]	0,15[0,15;0,16]**
Intertrabecular spaces (mm)			
5 day[1]	0,61[0,60;0,63]	0,61[0,59;0,63]	0,21[0,21;0,23]**
7 day[1]	0,43[0,42;0,45]	0,43[0,43;0,45]	0,20[0,19;0,21]**
Osteoblastic surface (%)			
5 day[1]	70,5[66,4;74,8]	64,3[62,0;67,1]**	25,3[24,0;26,4]**
7 day[1]	65,6[63,2;68,5]	59,2[57,9;60,2]**	21,8[20,2;23,5]**

Preprints (www.preprints.org) | NOT PEER-REVIEWED | Posted: 14 August 2023 doi:10.20944/preprints202308.1032.v1

	Erosed bone surface (%)		
5 day[1]	0,8[0,7;0,9]	1,0[0,9;1,1]**	12,0[11,3;13,3]**
7 day[1]	1,5[1,4;1,8]	1,9[1,6;2,1]**	7,9[7,7;8,0]**
	Interim dates		
	Numerical density of inflammatory infiltrate (unit/0.043 mm²)		
2 weeks[1]	26,8[24,2;28,5]	31,5[28,8;33,7]**	13,2[11,3;14,4]**
3 weeks[1]	17,2[15,8;19,9]	17,5[15,7;22,6]	6,2[5,7;7,1]**
	Volumetric density of bone tissue (BV %)		
2 weeks[1]	30,0[28,8;31,0]	28,3[25,8;29,9]**	65,0[63,8;66,5]**
3 weeks[1]	41,3[39,6;43,6]	38,6[36,1;40,2]**	67,8[67,0;69,3]**
4 weeks[1]	62,9[60,7;66,8]	60,9[58,0;62,0]**	66,5[64,3;68,1]**
	Trabeculae thickness (TT mm)		
2 weeks[1]	0,12[0,11;0,13]	0,11[0,10;0,12]*	0,16[0,16;0,17]**
3 weeks[1]	0,13[0,11;0,14]	0,12[0,12;0,13]*	0,15[0,14;0,16]**
4 weeks[1]	0,16[0,15;0,17]	0,14[0,13;0,15]*	0,16[0,15;0,17]**
	Intertrabecular spaces (ITS mm)		
2 weeks[1]	0,37[0,36;0,37]	0,39[0,38;0,40]**	0,22[0,22;0,24]**
3 weeks[1]	0,29[0,28;0,30]	0,30[0,29;0,31]**	0,24[0,23;0,25]**
4 weeks[1]	0,21[0,21;0,22]	0,22[0,21;0,22]**	0,21[0,20;0,22]
	Osteoblastic surface (OS %)		
2 weeks[1]	58,9[57,0;60,2]	49,9[49,5;50,4]**	13,1[12,4;13,7]**
3 weeks[1]	50,8[49,0;53,1]	42,0[39,6;43,9]**	9,1[8,4;9,8]**
4 weeks[1]	38,9[37,1;40,1]	36,0[34,7;37,0]**	7,2[6,3;7,8]**
	Erosed bone surface (ES %)		
2 weeks[1]	3,5[3,3;3,6]	3,9[3,7;3,9]**	6,1[5,5;6,9]**
3 weeks[1]	5,9[5,6;6,1]	6,4[6,1;6,6]**	2,9[2,7;3,0]**
4 weeks[1]	9,9[9,7;10,0]	10,7[10,5;11,1]**	1,3[1,2;1,4]**
	Late dates		
	Volumetric density of bone tissue (BV %)		
6 weeks[1]	67,5[65,4;68,6]	62,6[60,0;64,2]**	68,7[67,2;69,8]*
8 weeks	67,1[63,2;69,1]	65,2[63,4;69,2]	67,0[65,4;68,5]
10 weeks	67,3[65,1;68,2]	68,3[66,6;69,2]	67,8[66,3;69,2]
	Trabeculae thickness (TT mm)		
6 weeks	0,16[0,15;0,17]	0,16[0,15;0,16]	0,15[0,14;0,17]
8 weeks[1]	0,16[0,15;0,16]	0,15[0,14;0,16]*	0,15[0,14;0,15]

Preprints (www.preprints.org) | NOT PEER-REVIEWED | Posted: 14 August 2023 doi:10.20944/preprints202308.1032.v1

10 weeks	0,16[0,16;0,17]	0,16[0,15;0,17]	0,16[0,16;0,17]
	Intertrabecular spaces (ITS mm)		
6 weeks[1]	0,21[0,19;0,22]	0,21[0,20;0,22]	0,19[0,18;0,20]**
8 weeks[1]	0,20[0,19;0,20]	0,21[0,19;0,21]	0,19[0,18;0,19]**
10 weeks[1]	0,20[0,19;0,20]	0,22[0,21;0,23]	0,18[0,17;0,20]**
	Osteoblastic surface (OS %)		
6 weeks[1]	20,2[19,0;21,5]	16,4[14,9;18,0]**	4,0[2,8;4,7]**
8 weeks[1]	8,7[8,1;9,9]	8,4[7,1;9,6]	1,5[1,3;1,8]*
10 weeks[1]	3,6[2,8;4,0]	5,0[3,6;6,1]**	1,6[1,1;1,9]**
	Erosed bone surface (ES %)		
6 weeks[1]	4,8[4,6;4,9]	5,1[4,7;5,6]	0,8[0,7;0,9]**
8 weeks[1]	2,6[2,5;2,8]	3,1[3,0;3,4]**	0,7[0,5;0,9]**
10 weeks[1]	1,6[1,5;1,7]	1,3[1,2;1,4]**	0,9[0,8;0,9]**
	Bone growth rate (% per day)		
1-28 days	2,24[2,17;2,39]	2,17[2,07;2,21]**	
6-14 days	28,9 [26,3;30,4]	27,2 [25,2;29,0]**	
15-28 days	3,23[2,85;3,36]	3,15[2,64;3,52]	
29-70 days	0,96[0,92;0,97]	0,97[0,95;0,99]	
1-70 days (total)	0,94[0,82;1,25]	0,96[0,85;1,15]	

* Differences are reliable with the CH-SA-HA group ($p<0.05$) **Differences are reliable when compared with the CH-SA-HA group ($p<0.01$) [1]Significant differences in multiple comparisons ANOVA ($p<0.001$).

On the 2nd and 3rd weeks of the experiment, formed bone beams were visualized in the area of the inflicted defect, on the surfaces of which numerous osteoblasts were detected, mostly of a cubic shape (Figure A.2, B.2). The volume of surfaces of bone beams occupied by osteoblasts in preparations of 3 weeks was noticeably lower when compared with preparations of previous time intervals. In both study groups, few osteoclasts were detected with the formation of characteristic lacunae (Figure A.2). The structure of most bone beams was characterized by ordered fibers. The density of cellular infiltrate in comparison with the previous time intervals was noticeably lower among the dense connective tissue structures and was characterized by mild infiltration, mainly by histiocytes and fibroblasts. In the group of animals with CH-SA-HA implantation, diffusely distributed, finely dispersed amphophilic granules containing a polysaccharide construct were detected.

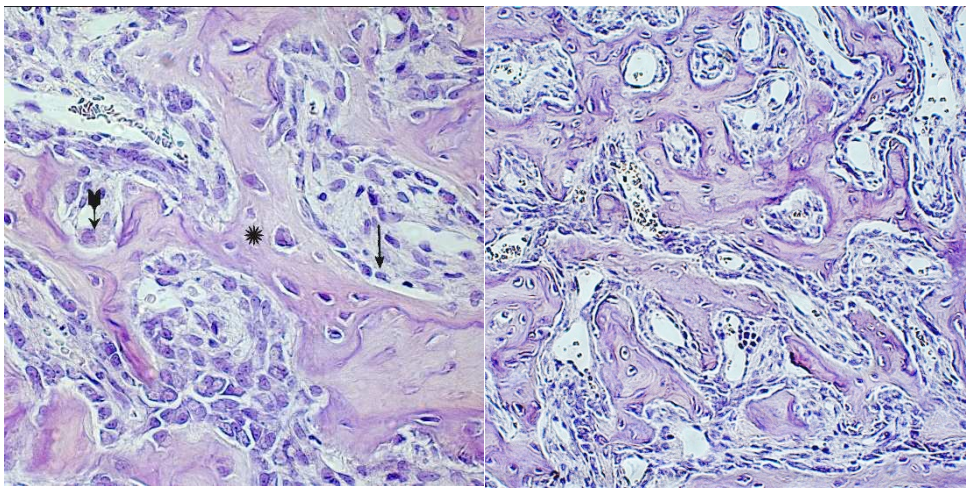

Preprints (www.preprints.org) | NOT PEER-REVIEWED | Posted: 14 August 2023 doi:10.20944/preprints202308.1032.v1

A.2 B.2

Figure 2. Changes in the area of the bone defect characterizing the active phase of bone tissue regeneration in healthy and experimental groups of rats: A.2 - CH-SA-HA group, 2nd week of the experiment. On the surface of the bone beams (*), multiple osteoblasts are visible (arrow), and a formed gap with an osteoclast is also visible (➸). Hematoxylin-eosin staining, magnification x400; B.2 - control group. 2nd week of the experiment, most of the surfaces of the bone beams are covered with osteoblasts. Coloring G-E, magnification x100.

By the end of 1 week after surgery, the volumetric density of bone tissue increases many times, both in the experiment and in the control. However, starting from the 2nd week, the value of BS in the experiment significantly exceeds the control results. In fact, in the first month of the experiment, the bulk of the newly formed bone tissue with high growth rates of the spongy and compact components is laid in the experiment (Table 1). A high inflammatory reaction in the intrinsic zone of the bone defect is combined with a low level of inflammation in the peripheral zone and a stable picture of bone tissue volume at a distance of 5 mm from the zone of inflammation in the first 6 weeks of the experiment ($p<0.01$). Filling the surface of the bony trabeculae with cell mass leads to thickening of the trabeculae and contraction of the intertrabecular spaces and the inactive free bone surface. In the first 2 weeks, the increase in the thickness of bone trabeculae in the experiment is 100%, in the control 83%. The walls of the bone cavity in the control after 3 weeks - in the form of thin bone beams with pronounced intertrabecular spaces and poor cell mass (Figure A.3). The 4th week in the experimental group shows a newly formed bone in the defect zone, a large proportion of the surfaces of the bone beams are already free from cells, which indicates a partial process of completion of osteogenesis. (Figure B.3). However, in almost all periods of registration, the spongy part of the bone wall of the defect in the experimental group was filled significantly higher with osteoblastic cell mass (Table 1). The analysis shows that after 4 weeks, a late final stage of bone resorption is formed, as indicated by a significantly higher number of osteoclastic type cells with the formation of lacunar surfaces. In the bones of the experimental group of animals, signs of small focal accumulations of the implanted polymer are preserved.

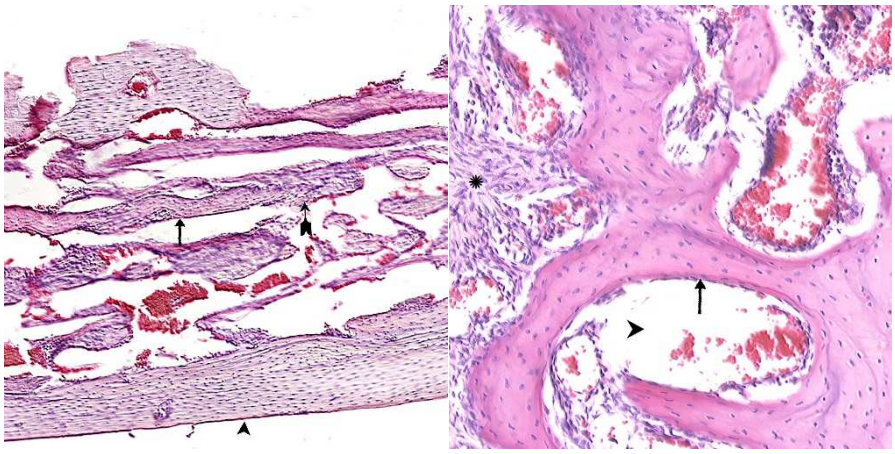

A.3 B.3

Figure 3. A.3 – The control group, 3rd week of the experiment, formed thin bone trabeculae in the area of the defect (↑) with pronounced intertrabecular spaces (➸), bone trabeculae are covered with cell mass (^), magnification x15; B.3 - CH-SA-HA group, 4 weeks. Visible bone beams with predominantly free surfaces (↑) and intertrabecular spaces (^), the adjacent peripheral area with the growth of maturing connective tissue (*). Hematoxylin-eosin staining, magnification x210.

During the 6th and 8th weeks, spongy bone tissue predominates at the defect site with oriented bone trabeculae, flattened osteoblasts and single osteoclasts. 6 weeks after implantation of the CH-SA-HA biopolymer, rare small-focal accumulations of amphophilic granules with graft remnants

Preprints (www.preprints.org) | NOT PEER-REVIEWED | Posted: 14 August 2023 doi:10.20944/preprints202308.1032.v1

were determined. After 8.10 weeks, foreign bodies were not detected. An important result is the active closure of a bone cavity of a critical size with full-fledged cancellous and compact bone (Figure 4).

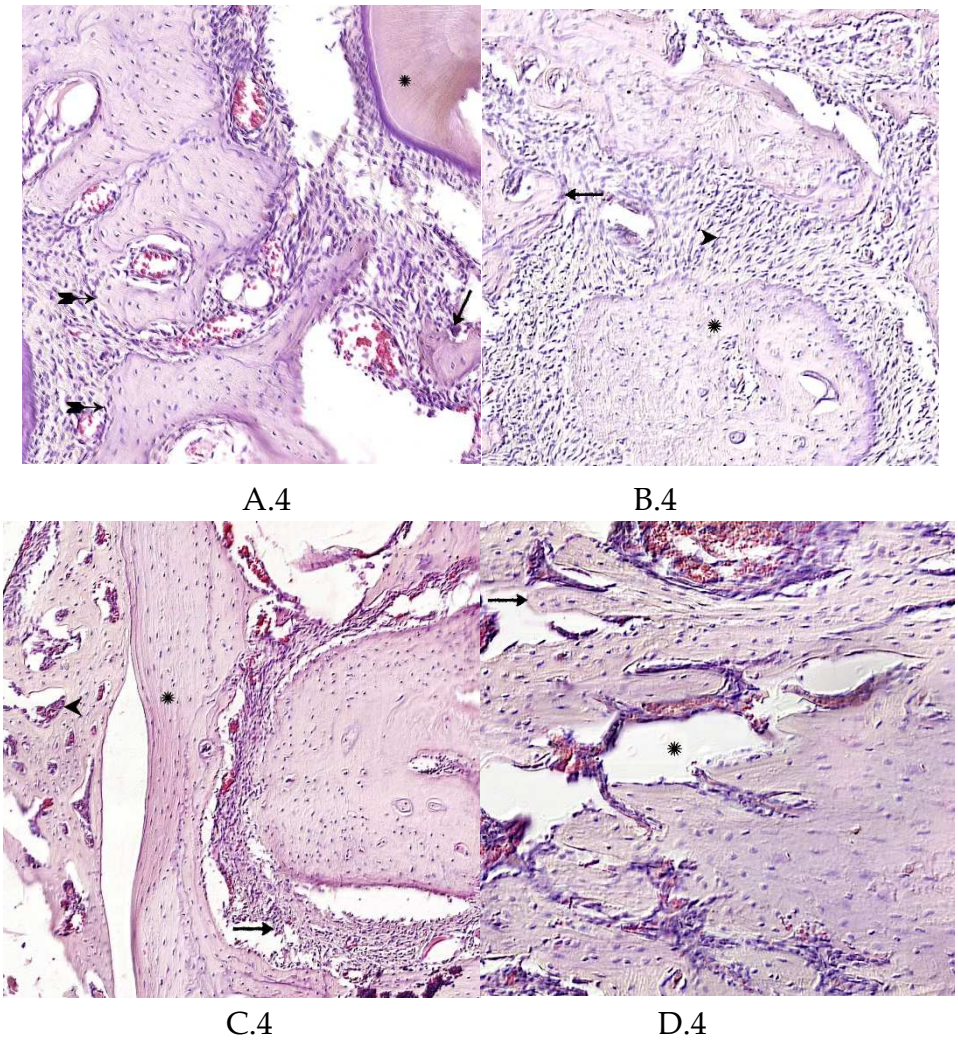

Figure 4. Late terms of reorganization of the bone cavity in the experimental group. A.4 - 6 weeks, oriented bone beams with a mass of flattened osteoblasts (➸), adjacent peripheral area with proliferation of maturing connective tissue, active endothelialization of bone regeneration, single osteoclasts (↑), organization of compact bone and periodontal ligament (*), x210 magnification ; B.4 - 8 weeks, large amount of spongy (tip) and compact (*) bone tissue with cellular reaction on the bone beams (arrow) and the formation of many micro-vessels, magnification 100; C.4 – experimental group, 10 weeks, signs of final reconstruction of the bone cavity, mature connective tissue in the border zone (↑), adjacent bone tissue (*) - reactive bone marrow structures (^), magnification. x150; D.4 – 10 weeks, the mandibular defect is closed by a compact bone, osteons are formed (↑), many Haversian canals with a vascular component (*). Hematoxylin-eosin staining.

The application of a large bone injury in the lower jaw triggers the mechanism of early bone resorption in both groups with an active osteoclastic reaction, especially at the periphery of the defect (Table 1), followed by active replacement with new bone. The activity of bone resorption in the peripheral zone exceeds 12-15 times when compared with the area of the bone defect. The control group of animals is characterized by a long reaction of bone destruction with a slower formation of spongy and especially compact bone ($p<0.01$). After 6 weeks, the activity of osteomalacia processes sharply and steadily decreases to its original value. Active early and prolonged (within 6 weeks) osteoblastic reaction in the experimental group provides early formation of the osteoid matrix, ready for the mineralization of new bone. The processes of osteoblastic reaction and osteoid formation proceed dynamically and synchronously (Figure A.5, A.6).

Preprints (www.preprints.org) | NOT PEER-REVIEWED | Posted: 14 August 2023 doi:10.20944/preprints202308.1032.v1

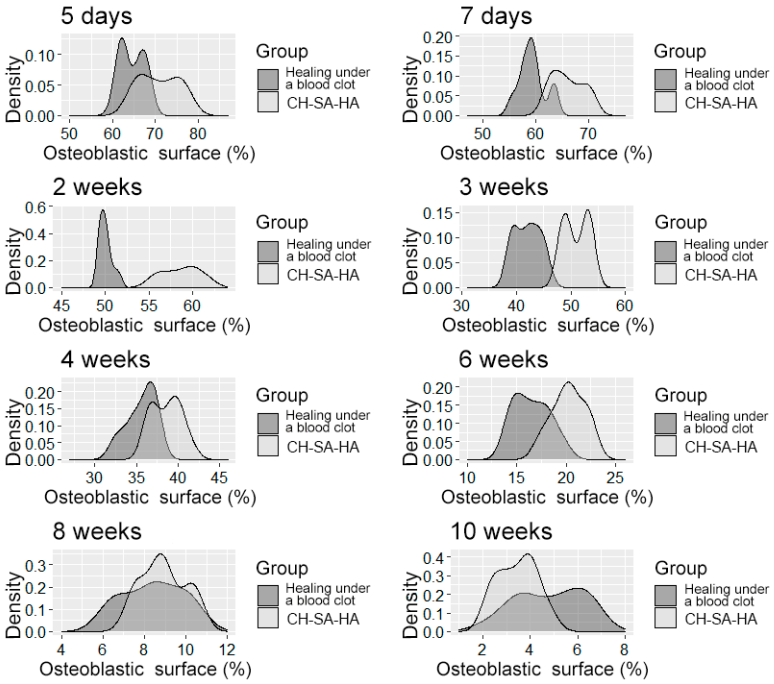

A.5

Figure 5. A- The density distribution of the variable is "osteoblast surface".

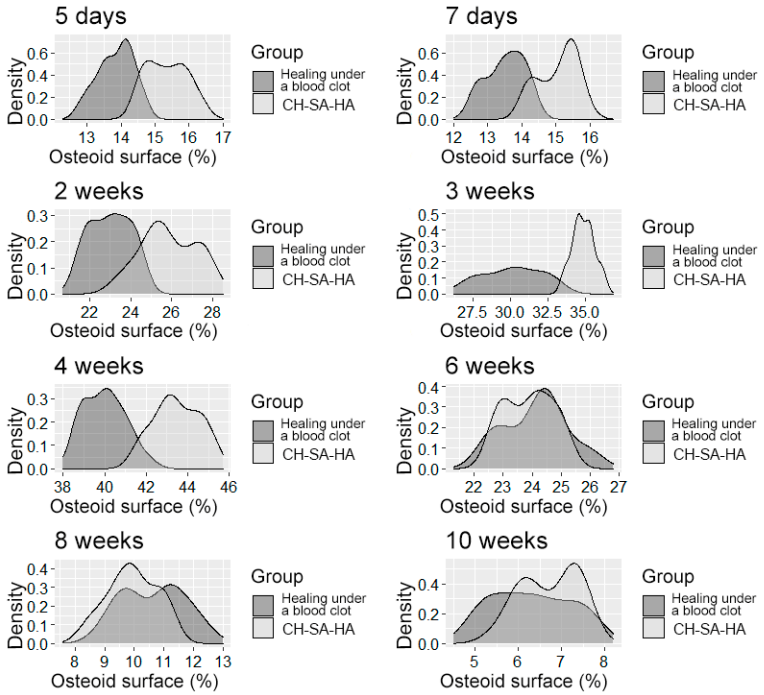

A.6

Figure 6. A - The distribution density of the variable is "osteoid surface".

It should be pointed out that the activity in the dynamics of osteogenesis in the control group is significantly lower than the results of the experiment. The inactive zone of the bone cavity walls (FS%) occupies a significant area during the first 6 weeks of the regeneration process (Figure A.7).

Preprints (www.preprints.org) | NOT PEER-REVIEWED | Posted: 14 August 2023 doi:10.20944/preprints202308.1032.v1

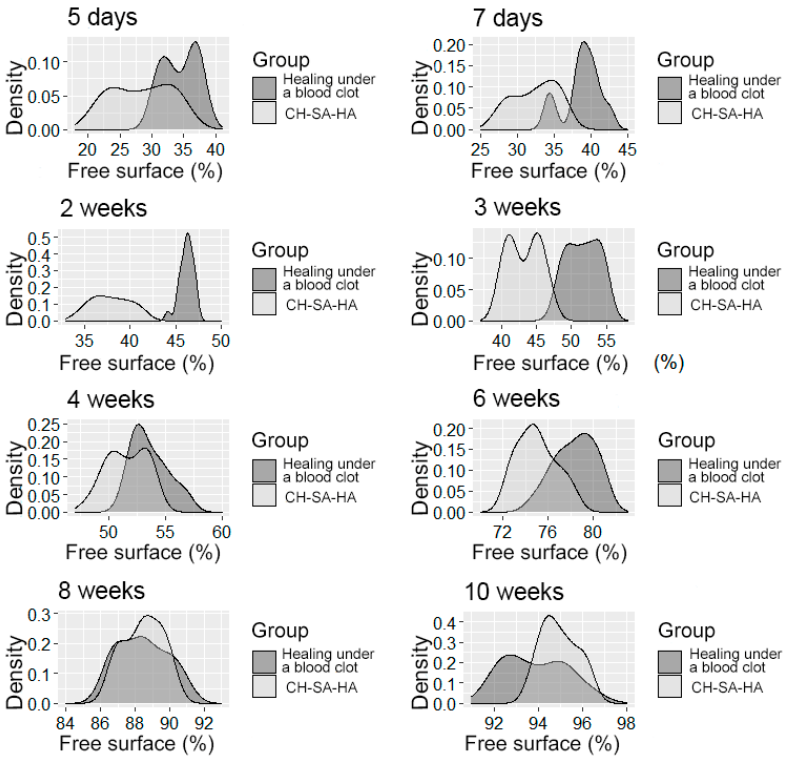

A.7

Figure 7. A- The distribution density of the variable is the "free surface" in the studied groups at different times of the experiment.

An important final result of bone defect regeneration is the rate of bone tissue growth as a percentage for 1 day. The results show that with an arbitrary choice of time intervals 1-28 days, 6-14 days, 15-28 days, 29-70 days, 1-70 days, the activity of osteogenesis processes changes significantly. One-way statistical analysis (ANOVA) established the significance ($p<0.01$) of the influence of the experimental period factor on the variable under consideration. Even though the growth rate for the entire period of the experiment (70 days) was 0.94% per day in the group with implanted CH-SA-HA biopolymer and 0.96% per day in the control group, a high rate of bone tissue growth in the focus regeneration was observed in the time interval of 6-14 days. In the group with implanted biopolymer, the growth rate was 28.9% per day, and in the control group this figure was 27.2% per day. Statistical analysis based on Welch's T-test showed that this difference was significant ($p<0.01$). Analysis over a randomly selected period of 1-28 days also revealed significant differences ($p<0.01$) in favour of the group of animals implanted with CH-SA-HA biopolymer (Figure A.8).

Preprints (www.preprints.org) | NOT PEER-REVIEWED | Posted: 14 August 2023 doi:10.20944/preprints202308.1032.v1

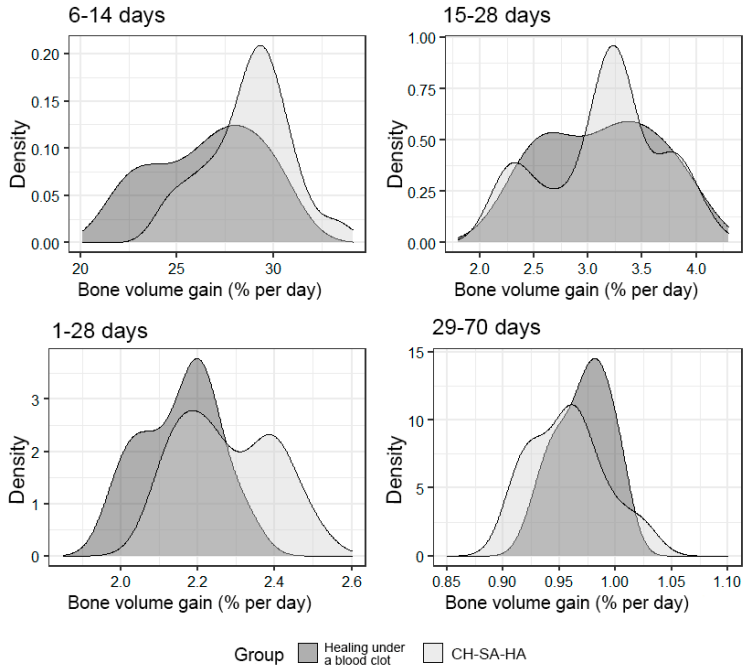

A.8

Figure 8. A - The density of the distribution of the variable - "increase in bone volume" in the study groups at randomly selected intervals of the experiment.

4. Summary

Thus, the early specialization of cells in the walls of bone defects and, ultimately, a rapid response to new bone formation with its reconstruction allowed the authors of the study to propose a technology for restoring bone tissue in the maxillofacial region with critical sizes of postoperative defects. It is important to point out that the implantation of the CH-SA-HA construct into a large bone cavity significantly reduces inflammatory infiltration in the injury zone in the early stages, and regeneration proceeds under favorable conditions compared to the control group of animals. Within 70 days of bone defect reconstruction, the most active periods of osteogenesis were revealed, in which the implant actively regulated the processes of osteoblastic and osteoclastic reactions, and reduced the inactive, cell-free bone surface in the early stages. It is important that the production of such products is a promising direction not only in maxillofacial surgery, but also in the field of dental transplantology, where a tight contact between implants and bone is required.

5. Discussion

Obtaining a morphological picture of early bone formation due to the active formation of the osteoid surface, starting from 5-7 days after surgery, and confirmation of this process during the first month after injury indicates the role of the polymer structure in the advanced regeneration of the cancellous part of the bone. The authors believe that the creation of specialized technologies and technical means for obtaining osteogenic matrices for direct transplantation into bone tissue defects in animals and humans is very important for subsequent widespread use in medical practice. Successfully constructed osteogenic matrices, when in contact with the wall of the bone cavity, are able to reduce or even exclude certain stages of osteogenesis, for example, the cartilaginous stage of development, and trigger the mechanisms of early bone formation. The absence of a well-perfused substrate in the affected area in the early stages after extensive trauma to the bone tissue, the lack of the ability of synthetic materials that do not contain growth factors and osteogenic cells to cover large bone defects of a critical size [20] is one of the main problems in the long-term restoration of the integrity of cancellous and compact bones. Preservation of the viability of the mass of cellular material over a large extent of the bone defect should consist of obtaining a highly vascularized module in an artificial matrix and creating conditions for its integration into a hard tissue. The formation of microvessels is the basis for the physiologically active process of bone formation [21]. Despite the

 doi:10.20944/preprints202308.1032.v1

successful solution of the issue of the beginning of early bone formation, the first stage of the process of reconstruction of the vascular network remains insufficiently understood from the point of view of the mechanism of contact interaction between the vascular endothelium and artificial or natural polymers. If polymer matrices in the form of nanoparticles are used (this design was used in the work of the authors), then this enhances the efficiency of the delivery of vector molecules to cells and leads to overexpression of angiogenesis molecules, enhances endothelial recruitment and new formation of blood microvessels [22]. Stimulation of proliferation and translation of the vascular endothelium occurs outside the vascular wall into the tissue compartment [23-25]. Using this postulate, it should be clarified that the formation of microvessels in the body of the matrix is an earlier stage of reconstruction, followed by osteogenesis [26–28]. At the same time, one of the important conditions for the rapid integration of building material is, in addition to degradation, high biocompatibility, the manifestation of its own angiogenic qualities, the ability to block polysaccharide and protein structures on the microbial cell surface, which provide transmembrane transport, and the ability to block pain conduction on somatic cells. These properties are known to be possessed by natural polysaccharide materials of cationic, anionic or amphoteric structure. Modern approaches to solving the problem of vascularization also include the introduction of low molecular weight serum growth factors into the injury zone (for example, the serum growth factors in cattle "adgelon" used in the work) based on a biodegradable polymer framework, which plays the role not only of a depot of dislocation of growth factors, but also of a program their prolonged elution as a result of a certain rate of polymer biodegradation. Dosed elution of growth factors from a modern polysaccharide matrix forms new capillaries [29]. Uncovering the mechanisms of the initial stages of angiogenesis will solve the problem of critical early osteogenesis. Thus, early endothelialization of the artificial matrix is a primary promising task and will mean the oriented sprouting of precursors or specialized cells, as well as signalling molecules of intercellular interaction, and, as a result, an active process of early osteogenesis [30]. Tight contact of the initially cell-free polysaccharide copolymer matrix with spongy and compact plates of the bone cavity with a certain filling of polymers with angiogenesis products triggers the process of matrix endothelization. Upon contact with the maternal vascular network, induced proliferation of the vascular endothelium and its translation into the subintimal zone occur, which culminates in an intensive neoplasm of microvessels. Under favourable conditions, this process captures the zone of the artificial matrix. The initial start of endothelialization ends with the rapid filling of the cell-free matrix with the vascular network. The osteoblastic and osteoclastic microenvironment of the vascular implant stimulates the rapid formation of cancellous and compact bone from the periphery to the centre of the implant. It is very important that the artificially created vascular network does not regress after the complete degradation of the implant. The use of sodium alginate in the work was based on the results of modern research on the use of this polymer for tissue engineering [31-33]. However, weak mechanical strength and low activity of cell binding, especially in the hydrated state [34], low thermal and electrical conductivity, and antibacterial activity during the creation of the polymer scaffold required the inclusion of other polymers in this design. The inclusion of other polymers or inorganic compounds in the alginate significantly improves the mechanical and functional properties of the new design. This is especially important when solving the problem of eliminating a bone tissue defect of a critical size. It has been shown that the inclusion of hydroxyapatite in scaffolds based on sodium alginate increases the stability of the scaffolds and opens access to the cell surface [35], improves biocompatibility, changes the microrelief of the matrix surface, and increases adhesion and migration of osteoblasts [36]. It has been shown [37] that scaffolds based on alginate and hydroxyapatite enhance the local elimination of a bone defect since they do not cause inflammatory effects. The inclusion of various amounts of hydroxyapatite or alginate in the overall design reduces the rate of degradation in tissues.

It is known that the use of a chitosan membrane as a single polymer leads to the formation of new bone and cementum in single-wall intraosseous defects in large experimental animals [38]. Physical or chemical synthesis with other polymers significantly increases the mechanical strength and elasticity of the hydrogel [39]. The mutual penetration of individual polymers with the formation of hydrogel networks reinforces the structure, which is considered one of the best technologies for obtaining a composite with high mechanical properties [40]. Such combined meshes were developed using alginate and chitosan [41] or hyaluronic acid [42,43] for the purpose of bone tissue bioengineering. If a combination of chitosan with an alginate–hydroxyapatite framework is obtained

[44–46], then the gel matrix is stabilized due to the formation of polyelectrolyte complexes. The complexes are formed as a result of a weak interaction of oppositely charged chemical groups of COO-alginate and NH3+ of chitosan. In addition, NH3+ groups can interact with PO43-hydroxyapatite groups, linking the framework together and forming a more compact structure. In this case, porosity and degradation rate decrease, and mechanical stability increases [47]. If we are talking about the destruction of periodontal tissues in the experiment, then filling a bone defect with a complex of chitosan with a polyanionic structure, for example, collagen [48], leads to inhibition of the apical migration of the epithelium and active formation of new bone and cementum. Such dynamics are due to the induction of the differentiation of mesenchymal cells into cementoblasts. The introduction of additional natural polysaccharide polymers into the structure leads to obtaining not only excellent mechanical strength, but, which is very important, to the active implementation of cellular functions such as adhesion, proliferation and differentiation. For example, a composite scaffold consisting of a combination of chitosan, alginate, hydroxyapatite, and cellulose nanocrystals possesses such properties, which is especially valuable for bone tissue engineering. Attention should be paid to the use of sulfated polysaccharides such as heparin in the preparation of functional copolymers. Three sulfo groups in the heparin molecule allow large rigid linear polymers to be converted into nanosized globules, which predetermines their high mobility in living animal tissues [7]. The high specific affinity of heparin for growth factors, for example, bFGF [49], is due to the presence of a mechanism of active electrostatic interaction between the negatively charged sulfate groups of heparin and the positively charged amino acid residues of the growth factor [50]. The high affinity of heparin for growth factors ensures high protein loading into the construct. The higher the growth factor loading, the higher the effect of angiogenesis. It has been established that bioactive growth factors must be slowly released from scaffolds to achieve long-term therapeutic effects [51]. Long-term dosed release into the medium, for example, of the main fibroblast growth factor (bFGF) significantly increases the angiogenic effect and capillary density in a short time [52,53]. However, this growth factor has a short half-life [54] and rapid diffusion from the injury site. Therefore, its practical application should be carried out in combination with a polysaccharide matrix. A copolymer alginate-chitosan structure containing additional anionic polysaccharides as a delivery system for growth factors can be a promising solution in the formation of a vascular bed not only in the bone cavity, but also in the polymer matrix proper.

Statement of Authorship: Patlataya, N. - participated in the design, participated in the acquisition of investments, drafted the manuscript, ensuring integrity and accuracy; Bolshakov I. - participated in the concept and design, participated in the acquisition of material and analysis, compiled the manuscript, critically edited the manuscript; Levenets A. - contributed to the idea, contributed to the interpretation of the results, critically revised the manuscript; Medvedeva N. - participated in the design, analysis and interpretation of the results of morphometric measurements, critically edited the manuscript; Cherkashina M. - professional English translation of medical information, preparation of a literature review for a specific project. All authors gave their final approval and agree to be accountable for all aspects of the work.

Acknowledgments: The authors express their gratitude to the staff of the Center for Collective Use of the Prof. V.F.Voino-Yasenetsky Krasnoyarsk State Medical University Ministry of Health of the Russian Federation for providing the laboratory conditions for the physical synthesis of a polyelectrolyte complex based on natural polysaccharides and performing experimental work on animals in accordance with international requirements. The authors express their gratitude to the staff of the morphological studies laboratory of the Krasnoyarsk Federal Cancer Center for their help in obtaining, scanning histological sections and obtaining high-resolution figures. The work was approved: complex scientific theme No. 01201362513 (2013/01/01 – 2021/01/01) "Fundamental and applied scientific and technical developments of nano-level biopolymer structures and technologies for their production for use in cell and tissue engineering in socially significant human diseases"; Section "Dentistry": Obtaining, testing and introduction into clinical practice of cell substrates for direct implantation into hard and soft tissues of the periodontium in order to reconstruct the tissues of the maxillofacial region, eliminate the causes of the formation of degeneration zones and the formation of periodontolysis zones; Research topic: "Restoration of the structure of the bone tissue of the maxillofacial region using polysaccharide polymers with extensive traumatic defects in conditions of sub-compensated diabetes mellitus." The implementation of the project was consulted on the basis of the Center for Collective Use scientific base Prof. V.F. Voino-Yasenetsky Krasnoyarsk State Medical University and the Federal Research Center "Krasnoyarsk Scientific Center of the Siberian Branch of the Russian Academy of Sciences" on the basis of agreement No. 1-2/1 of 10/23/2017 and No. 1-2/2 dated 10/23/2017 between the Regional State Autonomous Institution "Krasnoyarsk Regional Innovation and Technology Business Incubator" ("KRITBI") and FSBEI HE "Krasnoyarsk State Medical

University Prof. V.F. Voino-Yasenetsky Ministry Health of Russia, LLC "Bioimplant" (Krasnoyarsk) (General Director Bolshakov I.N.)(the agreement No. 2/t dated 09/13/2017).

Conflicts of Interest: The Authors declares that there is no conflict of interest.

Protocol of the Bioethical Commission for Working with Animals at the Local Ethics Committee of the Federal State Budgetary Educational Institution of Higher Education Prof. V.F. Voino-Yasenetsky Krasnoyarsk State Medical University" of the Ministry of Health of the Russian Federation (No1 November 30, 2017). The Application for Scientific Experimental Research has been provided in the following wording: To the chairman of the local ethics committee Prof. Demko I.V. from Prof. Department of Operative Surgery and topographic anatomy Bolshakov I.N.

Petition. In connection with the implementation of a complex scientific topic (headed by Prof. I. N. Bolshakov) No. 01201362513 (2013.01.01-2021.01.01) "Fundamental and applied scientific and technical development of nano- level biopolymer structures and technologies for their production for use in cellular and tissue engineering for socially significant human diseases "I ask permission to conduct experimental scientific work in the section of medicine" dentistry "on animals (white laboratory rats) according to the research protocol, research objectives, design, analysis plan). The study protocol was registered with the local ethical committee of the Federal State Budgetary Educational Institution of Higher Education Prof. V.F. Voino-Yasenetsky Krasnoyarsk State Medical University" of the Ministry of Health of the Russian Federation. The protocol was prepared and registered before the research. The maintenance and disposal of experimental animals corresponds to the sanitary and epidemiological standard established for an educational and scientific institution in the Russian Federation.

References

1. Shaykhaliev,A.I.; Stretskiy, G.M.; Krasnov, M.S.; Rybakova, E.Yu.; Tikhonov, V.E.; Arazashvili, L.D.; Gevorkov, G.L.; Yamskova, V.P.; Yamskov, I.A. Use of materials with bioregulatory peptide complex, affecting osteoreparation process (the results of preclinical tests). Russian Dental Journal. **2014**, 18(4), 12-16; https://doi.org/10.17816/dent-2014.18.4.
2. Lou, X. Induced pluripotent stem cells as a new strategy for osteogenesis and bone regeneration. Stem Cell Rev. Rep. **2015**, 11(4), 645-651; DOI:10.1007/s12015-015-9594-8.
3. Raposo-Amaral, C.E.; Bueno, D.F.; Almeida, A.B.; Jorgetti, V.; Costa, C.C.; Gouveia, C.H.; Vulcano, L.C.; Fanganiello, R.D.; Passos-Bueno, M.R.; Alonso, N. Is bone transplantation the gold standard for repair of alveolar bone defects? J. Tissue Eng. **2014**, 5, 2041731413519352; DOI:10.1177/2041731413519352.
4. Shanbhag, S.; Pandis, N.; Mustafa, K.; Nyengaard, J.R.; Stavropoulos, A. Alveolar bone tissue engineering in critical-size defects of experimental animal models: a systematic review and meta-analysis. J. Tissue Eng. Regen. Med. **2017**, 11(10), 2935-2949; DOI:10.1002/term.2198.
5. Khan,F.; Tanaka, M.; Rafi, S. Ahmad fabrication of polymeric biomaterials: a strategy for tissue engineering and medical devices. J. Mater. Chem. B. **2015**, 3, 8224-8249; DOI:10.1039/C5TB01370D.
6. Henkel, J.; Woodruff, M.A.; Epari, D.R.; Steck, R.; Glatt, V.; Dickinson, I.C.; Choong, P.F.M.; Schuetz, M.A.; Hutmacher, D.W. Bone regeneration based on tissue engineering conceptions – a 21st century perspective. Bone Res. **2013**, 3, 216-248; DOI:10.4248/BR201303002.
7. Bolshakov, I.N.; Levenetz, A.A.; Furtsev, T.V.; Kotikov, A.R.; Patlataya, N.N.; Ryaboshapko,E.I.; Dmitrienko, A.E.; Nikolaenko, M.M.; Matveeva, N.D.; Ibragimov, I.G. Experimental Reconstruction of Critical Size Defect of Bone Tissue in the Maxillofacial Region When Using Modified Chitosan. Biomed. Transl. Sci. **2022**, l.2(1), 1-8; DOI:10.33425/2768-4911.1024.
8. Bolshakov, I.N.; Gornostaev, L.M.; Fominykh, O.I.; Svetlakov, A.V. Synthesis, Chemical and Biomedical Aspects of the Use of Sulfated Chitosan. Polymers. **2022**, 14(6), 1-27; DOI:10.3390/polym14163431.
9. Li, Y.; Kim, J.H.; Choi, E.H.; Han, I. Promotion of osteogenic differentiation by non-thermal biocompatible plasma treated chitosan scaffold. Sci. Rep. **2019**, 9(1), 3712; DOI: 10.1038/s41598-019-40371-6.
10. Carletti, E.; Motta, A.; Migliaresi, C. Scaffolds for tissue engineering and 3D cell culture. Methods Mol. Biol. **2011**, 695, 17-39; DOI: 10.1007/978-1-60761-984-0_2.
11. Jiang,T.; Khan, Y.; Nair, L.S.; Abdel-Fattah, W.I.; Laurencin, C.T. Functionalization of chitosan/poly(lactic acid-glycolic acid) sintered microsphere scaffolds via surface heparinization for bone tissue engineering. J. Biomed. Mater. Res. A. **2010**, 93(3), 1193-1208; DOI: 10.1002/jbm.a.32615.
12. Sukpaita, T.; Chirachanchai, S.; Suwattanachai, P.; Everts, V.; Pimkhaokham, A.; Ampornaramveth, R.S. In vivo bone regeneration induced by a scaffold of chitosan/dicarboxylic acid seeded with human periodontal ligament cells. Int. J. Mol. Sci. **2019**, 20(19), 4883; DOI: 10.3390/ijms20194883.
13. Dhandayuthapani, B.; Yoshida, Ya.; Maekawa, T.; Kumar, D.S. Polymeric scaffolds in tissue engineering application: a review. Int. J. Polymer Sci. **2011**; Article ID 290602:1-19; DOI:10.1155/2011/290602.

14. Chatzipetros, E.; Christopoulos, P.; Donta, C.; Tosios, K.-I.; Tsiambas, E.; Tsiourvas, D.; Kalogirou, E.-M.; Tsiklakis, K. Research application of nano-hydroxyapatite/chitosan scaffolds on rat calvarial critical-sized defects: a pilot study. Med. Oral Patol. Oral Cir. Bucal. **2018**, 23(5), e625-e632; DOI:10.4317/medoral.22455.
15. La, W.-G.; Jang, J.; Kim, B.S.; Lee, M.S.; Cho, D.-W.; Yang, H.S. Systemically replicated organic and inorganic bony microenvironment for new bone formation generated by a 3D printing technology. RSC Adv. **2016**, 6, 11546-11553; DOI:10.1039/C5RA20218C.
16. Ko, H.F.; Sfeir, C.; Kumta, P.N. Novel synthesis strategies for natural polymer and composite biomaterials as potential scaffolds for tissue engineering. Philos. Trans. A Math. Phys. Eng. Sci. **2010**, 28, 368(1917), 1981-1997; DOI:10.1098/rsta.2010.0009.
17. Vukajlovic, D.; Parker, J.; Bretcanu, O.; Novakovic, K. Chitosan based polymer/bioglass composites for tissue engineering applications. Mater. Sci. Eng. C Mater. Biol. Appl. **2019**, 96, 955-967; DOI: 10.1016/j.msec.2018.12.026.
18. Kirichenko, A.K.; Patlataya, N.N.; Sharkova, A.F.; Pevnev, A.A.; Kontorev, K.V.; Shapovalova, O.V.; Gorban, M.E.; Bolshakov, I.N. Pathomorphism of Limb Major Vessels in Experimental Atherogenic Inflammation. The Role of Adventitial Intimal Relations. Review. Modern Technologies in Medicine. **2017**, 9(3), 157-163; https://doi.org/10.17691/stm2017.9.3.20.
19. Tumshevits, O.N.; Bolshakov, I.N.; Belousova, Yu.B.; Zykova, L.D.; Tumshevits, V.O. Method for treatment of periodontitis with insulin-dependent diabetes mellitus with "HAG-BOL" drugs. Patent RF No 2309748, 01/10/2006.
20. Lovett, M.; Lee, K.; Edwards, A.; Kaplan, D.L. Vascularization strategies for tissue engineering, Tissue Eng. Part B Rev. **2009**, 15(3), 353–370; DOI: 10.1089/ten.TEB.2009.0085
21. Hasegawa, T.; Yamamoto, T.; Tsuchiya, E.; Hongo, H.; Tsuboi, K.; Kudo, A.; Abe, M.; Yoshida, T.; Nagai, T.; Khadiza, N.; Yokoyama, A.; Oda, K.; Ozawa, H.; de Freitas, P.H.L.; Li, M.; Amizuka, N. Ultrastructural and biochemical aspects of matrix vesiclemediated mineralization. Jpn. Dent. Sci. Rev. **2017**, 53, 34–45; DOI: 10.1016/j.jdsr.2016.09.002.
22. Thomas, A.M.; Gomez, A.J.; Palma, J.L.; Yap, W.T.; Shea, L.D. Heparin-chitosan nanoparticle functionalization of porous poly(ethylene glycol) hydrogels for localized lentivirus delivery of angiogenic factors. Biomaterials. **2014**, 35(30), 8687-8693; DOI:10.1016/j.biomaterials.2014.06.027.
23. Sivaraj, K.K.; Adams, R.H. Blood vessel formation and function in bone. Development. **2016**, 143(15), 2706-2715; DOI: 10.1242/dev.136861
24. Li, H.; Chang, J. Stimulation of proangiogenesis by calcium silicate bioactive ceramic. Acta Biomater. **2013**, 9(2), 5379–5389; DOI: 10.1016/j.actbio.2012.10.019
25. Gorustovich, A.A.; Roether, J.A.; Boccaccini, A.R. Effect of bioactive glasses on angiogenesis: A Review of in vitro and in vivo evidences, Tissue Eng. Part B Rev. **2010**, 16(2), 199–207; DOI: 10.1089/ten.TEB.2009.0416.
26. Kuttappan, S.; Mathew, D.; Jo, J.-I.; Tanaka, R.; Menon, D.; Ishimoto, T.; Nakano, T.; Nair, S.V.; Nair, M.B.; Tabata, Y. Dual release of growth factor from nanocomposite fibrous scaffold promotes vascularisation and bone regeneration in rat critical sized calvarial defect. Acta Biomater. **2018**, 78, 36–47; DOI: 10.1016/j.actbio.2018.07.050.
27. Sivaraj, K.K.; Adams, R.H. Blood vessel formation and function in bone, Development. **2016**, 143(15), 2706-2715; DOI: 10.1242/dev.136861.
28. Nguyen, L.H.; Annabi, N.; Nikkhah, M.; Bae, H.; Binan, L.; Park, S.; Kang, Y.; Yang, Y.; Khademhosseini, A. Vascularized bone tissue engineering: approaches for potential improvement, Tissue Eng. Part B Rev. **2012**, 18, 363–382; DOI: 10.1089/ten.TEB.2012.0012.
29. Sheridan, M.H.; Shea, L.D.; Peters, M.C.; Mooney, D.J. Bioabsorbable polymer scaffolds for tissue engineering capable of sustained growth factor delivery. J. Control Release. **2000**, 64(1-3), 91-102; DOI: 10.1016/s0168-3659(99)00138-8.
30. Amaral, I.F.; Neiva, I.; da Silva, F.F.; Sousa, S.R., Piloto, A.M.; Lopes, C.D.F.; Barbosa, M.A.; Kirkpatrick, C.J.; Pego, A.P. Endothelialization of chitosan porous conduits via immobilization of a recombinant fibronectin fragment (rhFNIII(7-10)). Acta Biomaterialia. **2013**, 9(3), 5643-5652; DOI: 10.1016/j.actbio.2012.10.029.
31. Liu, S.; Hu, Y.; Zhang, J.; Bao, S.; Xian, L.; Dong, X.; Zheng, W.; Li, Y.; Gao, H.; Zhou, W. Bioactive and biocompatible macroporous scaffolds with tunable performances prepared based on 3D printing of the pre-crosslinked sodium alginate/hydroxyapatite hydrogel ink. Macromol. Mater. Eng. **2019**, 304, 1800698; https://doi.org/10.1002/mame.201800698.
32. Sancilio, S.; Marsich, E.; Schweikl, H.; Cataldi, A.; Gallorini, M. Redox control of IL-6-mediated dental pulp stem-cell differentiation on alginate/hydroxyapatite biocomposites for bone ingrowth. Nanomaterials (Basel). **2019**, 9(12), 1656; DOI:10.3390/nano9121656.
33. Sumayya, A.S.; Muraleedhara Kurup, G. Marine macromolecules cross-linked hydrogel scaffolds as physiochemically and biologically favorable entities for tissue engineering applications. J. Biomater. Sci. Polym. Ed. **2017**, 28, 807–825; DOI: 10.1080/09205063.2017.1303119.

34. Li, Z.; Liao, Y.; Li, D.; Li, D.; Wang, H.; Sun, X.; Chen, X.; Yan, H.; Lin, Q. Design and properties of alginate/gelatin/cellulose nanocrystals interpenetrating polymer network composite hydrogels based on in situ cross-linking. Research Square, **2022**, 1-27, https://doi.org/10.21203/rs.3.rs-2215053/v1.
35. Filardo, G.; Perdisa, F.; Gelinsky, M.; Despang, F.; Fini, M.; Marcacci, M.; Parrilli, A.P.; Roffi, A.; Salamanna, F.; Sartori, M.; Schütz, K.; Kon, E. Novel alginate biphasic scaffold for osteochondral regeneration: An in vivo evaluation in rabbit and sheep models. J. Mater. Sci. Mater. Med. **2018**, 29(6), 74; DOI:10.1007/s10856-018-6074-0.
36. Torres, A.L.; Gaspar, V.M.; Serra, I.R.; Diogo, G.S.; Fradique, R.; Silva, A.P.; Correia, I.J. Bioactive polymeric–ceramic hybrid 3D scaffold for application in bone tissue regeneration. Mater. Sci. Eng. C **2013**, 33, 4460–4469; DOI: 10.1016/j.msec.2013.07.003.
37. Mahmoud, E.; Sayed, M.; El-Kady, A.M.; Elsayed, H.; Naga, S. In vitro and in vivo study of naturally derived alginate/hydroxyapatite bio composite scaffolds. Int. J. Biol. Macromol. **2020**, 165, 1346–1360; DOI: 10.1016/j.ijbiomac.2020.10.014.
38. Yeo, Y.J.; Jeon, D.W.; Kim, C.S.; Choi, S.H.; Cho, K.S.; Lee, Y.K.; Kim, C.-K. Effects of chitosan nonwoven membrane on periodontal healing of surgically created one-wall intrabony defects in beagle dogs. J. Biomed. Mater. Res. B Appl. Biomater. **2005**, 72, 86–93; DOI:10.1002/jbm.b.30121.
39. Waters, D.J.; Engberg, K.; Parke-Houben, R.; Ta, C.N.; Jackson, A.J.; Toney, M.F.; Frank, C.W. Structure and mechanism of strength enhancement in interpenetrating polymer network hydrogels. Macromolecules. **2011**, 44, 5776-5787; dx.doi.org/10.1021/ma200693e.
40. Darnell, M.; Sun, J.; Mehta, M.; Johnson, C.; Arany, P.R.; Suo, Z.; Mooney, D.J. Performance and biocompatibility of extremely tough alginate/polyacrylamide hydrogels. Biomaterials. **2013**, 34, 8042-8048; DOI: 10.1016/j.biomaterials.2013.06.061.
41. TIğlI, R.S.; Gumüşderelioğlu, M. Evaluation of alginate-chitosan semi IPNs as cartilage scaffolds. J. Mater. Sci. Mater. Med. **2009**, 20, 699–709; DOI:10.1007/s10856-008-3624-x.
42. Matricardi, P.; Di Meo, C.; Coviello, T.; Hennink, W.E.; Alhaique, F. Interpenetrating polymer networks polysaccharide hydrogels for drug delivery and tissue engineering. Adv. Drug Deliv. Rev. **2013**, 65,1172–1187; DOI:10.1016/j.addr.2013.04.002.
43. Venkatesan, J.; Bhatnagar, I.; Manivasagan, P.; Kang, K..-H.; Kim, S.-K.) Alginate composites for bone tissue engineering: A review. Int. J. Biol. Macromol. **2015**, 72, 269-281; DOI:10.1016/j.ijbiomac.2014.07.008.
44. Shchipunov, Y.A.; Postnova, I. Formation of calcium alginate-based macroporous materials comprising chitosan and hydroxyapatite. Colloid J. **2011**, 73, 565–574; DOI: 10.1134/S1061933X11040132.
45. Sharma, C.; Dinda, A.K.; Potdar, P.D.; Chou, C.-F.; Mishra, N.C. Fabrication and characterization of novel nano-biocomposite scaffold of chitosan–gelatin–alginate–hydroxyapatite for bone tissue engineering. Mater. Sci. Eng. C **2016**, 64, 416–427; DOI:10.1016/j.msec.2016.03.060.
46. Liu, D.; Liu, Z.; Zou, J.; Li, L.; Sui, X.; Wang, B.; Yang, N.; Wang, B. Synthesis and characterization of a hydroxyapatite-sodium alginate-chitosan scaffold for bone regeneration. Front. Mater. **2021**, 8, 69; DOI:10.3389/fmats.2021.648980.
47. Sharma, C.; Dinda, A.K.; Potdar, P.D.; Chou, C.-F.; Mishra, N.C. Fabrication and characterization of novel nano-biocomposite scaffold of chitosan–gelatin–alginate–hydroxyapatite for bone tissue engineering. Mater. Sci. Eng. C **2016**, 64, 416–427; DOI:10.1016/дж.мсек.2016.03.060.
48. Park, J.S.; Choi, S.H.; Moon, I.S.; Cho, K.S.; Chai, J.K.; Kim, C.K.. Eight-week histological analysis on the effect of chitosan on surgically created one-wall intrabony defects in beagle dogs. J. Clin. Periodontol. **2003**, 30, 443–53; DOI:10.1034/j.1600-051X.2003.10283.x.
49. Lu, Q.; Li, M.Y.; Zou,; Cao, T. Delivery of basic fibroblast growth factors from heparinized decellularized adipose tissue stimulates potent *de novo* adipogenesis J. Control. Release. **2014**, 174, 43-50; https://doi.org/10.1016/j.jconrel.2013.11.007.
50. Shen , H.; Hu, X.; Yang, F.; Bei, J.; Wang, S. Cell affinity for bFGF immobilized heparin-containing poly(lactide-co-glycolide) scaffolds. Biomaterials. **2011**, 32(13), 3404-3412; DOI:10.1016/j.biomaterials.2011.01.037.
51. Minardi, S.; Pandolfi, L.; Taraballi, F.; Wang, X.; De Rosa, E.; Mills, Z.D.; Liu, X.; Ferrari, M.; Tasciotti. E. Enhancing Vascularization through the Controlled Release of Platelet-Derived Growth Factor-BB. ACS Appl. Mater. Interfaces. **2017**, 9(17),14566-14575; DOI:10.1021/acsami.6b13760.
52. Hurtado, A.; Aljabali, A.A.A.; Mishra, V.; Tambuwala, M.M.; Serrano-Aroca, Á. Alginate: Enhancement Strategies for Advanced Applications. Int. J. Mol. Sci. **2022**, 23(9), 4486; DOI:10.3390/ijms23094486.
53. Ho, Y.C.; Mi, F.L.; Sung, H.W.; Kuo, P.L. Heparin-functionalized chitosan-alginate scaffolds for controlled release of growth factor. Int. J. Pharm. **2009**, 376(1-2), 69-75; DOI:10.1016/j.ijpharm.2009.04.048.
54. Lazarous, D.F.; Unger, E.F.; Epstein, S.E.; Stine, A.; Arevalo, J.L.; Chew, E.Y.; Quyyumi. A.A. Basic fibroblast growth factor in patients with intermittent claudication: results of a phase I trial. J. Am. Coll. Cardiol. **2000**,36(4),1239-1244; DOI:10.1016/s0735-1097(00)00882-2.